POAC '99
Espoo, Finland

Proceedings of the 15th
International Conference on
Port and Ocean Engineering
under Arctic Conditions

SHIP'S RIDGE RESISTANCE IN MODEL ICE

T. Leiviskä
Helsinki University of Technology, Ship Laboratory, Finland

ABSTRACT

A study of ship's ridge resistance at model scale is presented in this paper. The partitioning of ridge resistance between components of resistance for the ship's bow and the parallel mid-body as well as definition of the magnitude of these components were the main purposes of the study. An idealised ridge resistance graph that roughly corresponds to a ship's resistance graph is also introduced.

1 INTRODUCTION

All Finnish ports are surrounded by ice for a few months almost every winter. To make sure that the ships are able to operate during the wintertime the ice-navigation circumstances must be studied continuously. Ice ridges are the most difficult obstacles for ships to encounter and they cause a great increase in operation time. Though the proportion of ice ridges of the whole ice cover is not very large by area, by mass it can be even one third of the total ice mass (Leppäranta et al. 1991). The winter navigation research would be easier if we knew which components make up the ridge resistance and what are the circumstances that affect these components.

This paper presents results from model tests performed to study ridge resistance of ships. The maximum resistance and the proportions of the resistance components were also compared to an existing ridge resistance formula to clarify its accuracy. Here the term "ridge resistance" includes all the resistance components existing when the ship crosses a ridge: the pure ridge resistance, the open water resistance and the resistance caused by the consolidated layer as well as the effect of velocity. Also open water tests were performed and the open water resistance was found to be less than 2.5 % of the ridge resistance depending on the model velocity.

1.1 Description of ridge penetration event

In an idealised model, the penetration into a ridge can be divided into several phases, which depend on the ship's location in the ridge. In turn the resistance can be defined as a function of the penetration distance. In Figure 1 the penetration event has been divided into nine phases. For simplification the cross-sectional area of the ridge has been thought of as a rectangle whose height is greater than the model's draft. This kind of ridge resembles the model ice ridges of this work. The determination of the phases is based on the length of the bow, parallel mid-body and ridge as follows. 1) The stem encounters the ridge. 2) The whole stem is inside the ridge. 3) The parallel mid-body encounters the ridge. 4) The whole bow is inside the ridge. 5) The whole ship is inside the ridge. 6) The stem begins to come out of the ridge. 7) The whole of the stem is out of the ridge. 8) The parallel mid-body begins to come out of the ridge. 9) The whole bow is out of the ridge. 10) The whole ship is out of the ridge.

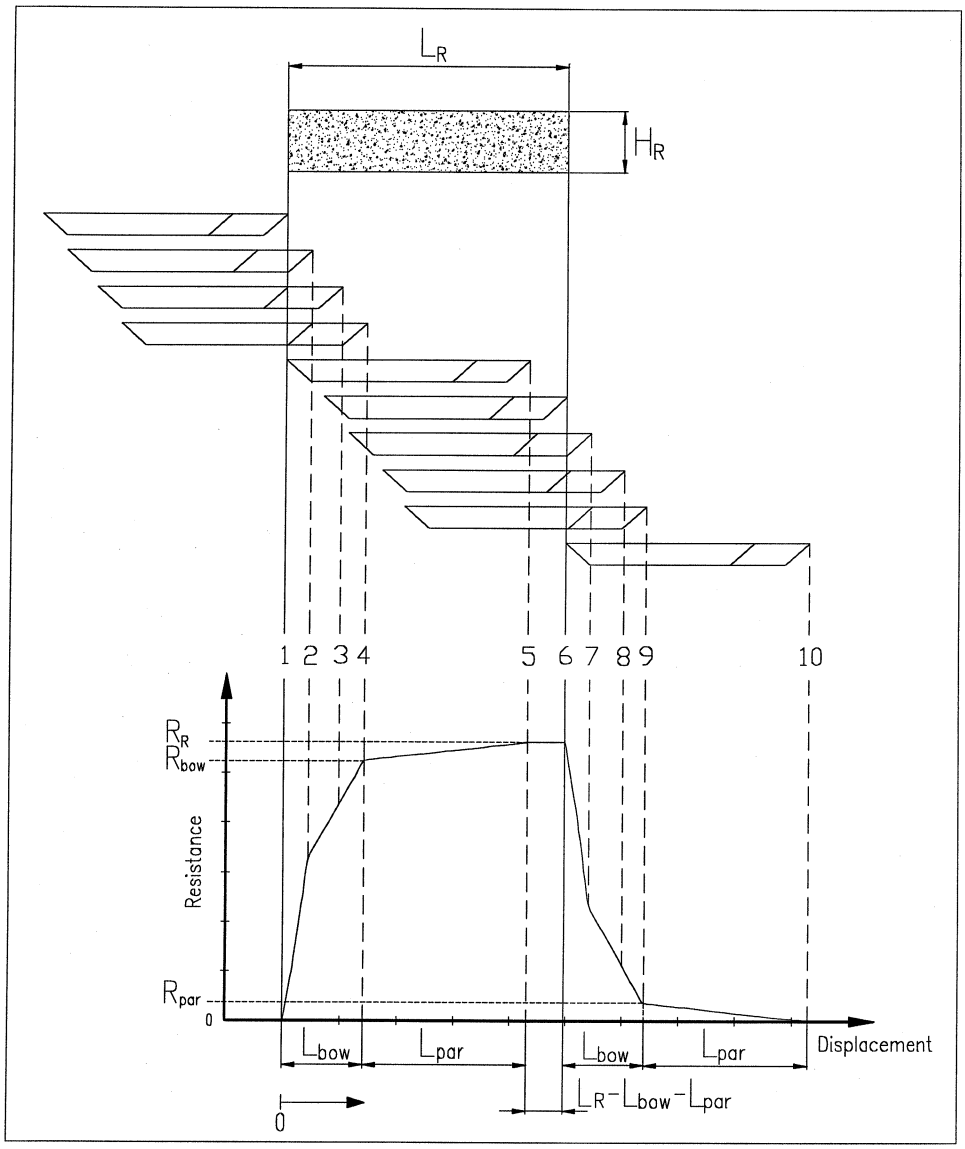

Figure 1: The nine phases of a penetration event.

The total ridge resistance R_R consists of the components for ship's bow R_{bow} and parallel mid-body R_{par}. R_{bow} is a function of ship's breath B(x), draught T(x) and ridge thickness H(x), where B(x) becomes B when the whole bow is inside the ridge and T(x) becomes T when the stem is inside the ridge. In this study ridge thickness H(x) was constant. R_{par} depends on the contact area of ice and the parallel mid-body.

It is not necessarily appropriate to divide the event into so many phases because the changes in resistance in points 2 and 7 in Figure 1 turned out to be rather difficult to distinguish in the model test results. That's why it is more appropriate to divide the penetration event only into five phases. 1) The bow is penetrating into the ridge. 2) The bow is inside the ridge and the parallel mid-body is penetrating into the ridge. 3) The whole ship is inside the ridge. 4) The bow is coming out of the ridge. 5) The bow is out of the ridge and the parallel mid-body is coming out of the ridge.

2 EXPERIMENTAL

The model tests were performed in the ice tank of the Ship Laboratory at the Helsinki University of Technology. The tank is a 40 m x 40 m water basin equipped with a cooling system and an xy-carriage. Water depth is 2.8 m. The x-carriage, or bridge, has a span of 40 meters and the smaller y-carriage hangs under it. The model ice currently used is granular fine-grained ice (Li and Riska, 1996). The ice is produced by spraying a mixture of ethanol and water into air from nozzles mounted on the x-carriage which is moving at a constant velocity back and forth across the basin. When the desired model ice thickness is reached the spraying is stopped and the ice is left to harden in about -15°C. The flexural and crushing strengths and the Young's modulus were measured before the tests. The strengths were determined from cantilever beam tests and the Young's modulus by the plate deflection method.

The used model scale in the tests was 1:20. Then the ice thickness of 40 mm corresponded to 0.8 m in full scale and was thick enough for ridges about the same thickness as the draft of the ship model. The model ice ridges were manufactured by breaking a level ice sheet into pieces and then pushing them into a long pile. The size of the ice pieces was approximately 0.1 x 0.1 m, which corresponds to a 2.0 x 2.0 m piece in full scale. A ridge manufactured this way is relatively monotonous with respect to thickness and resembles a ridge field or several ridges one after another. Two ridge thicknesses were used. The first four ridges were approximately as thick as the draft of the ship model, 0.37 m, and the last two ridges were 0.25...0.30 meters thick. The lengths of the ridges were approximately 4.5 meters for the thicker ridges and 5.5 meters for the thinner ridges. The average ridge profiles are shown in Figure 2.

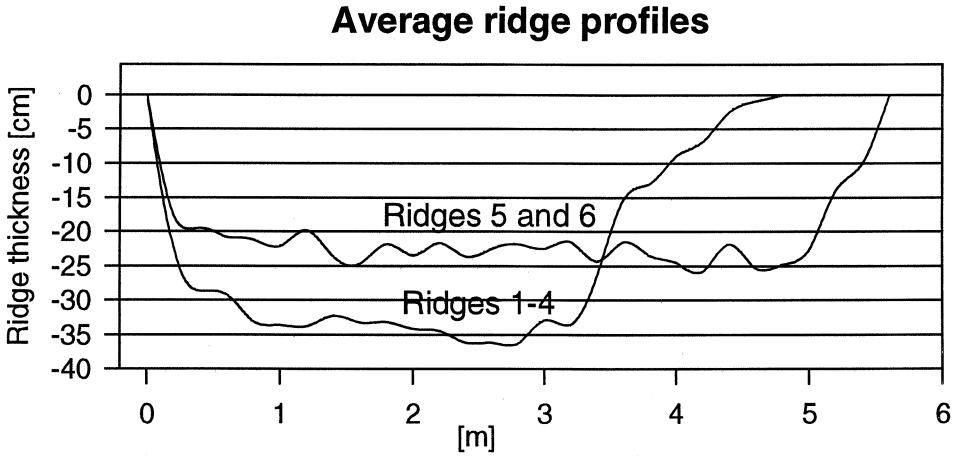

Figure 2: Ridge profiles

The effect of the consolidated layer was studied by freezing the ridges between the tests. To avoid the formation of solid ice between the ice blocks, an approximately 20 mm thick layer was sprayed on the ridge before the consolidation. Only one ridge was consolidated without spraying. The dependency of velocity was studied in the first two ridges with three different model speeds; 0.01, 0.23 and 0.46 m/s. In all other tests the speed was 0.23 m/s.

The ship model used in these tests was a model of a tanker without a bulbous bow. The tests were conducted as towing tests and only the towing force and the position of the model were measured. No rudders or propellers were installed. The main dimensions of the model were:

L_{wl} = 4.92 m
B = 0.90 m
T = 0.37 m

The model was towed trough the ridge in three different locations as illustrated in Figure 3. The model encountered the ridge from open water and there was a pre-sawn opening in the ice behind the ridge on each towing line so that the model also arrived at open water after the ridge. Between the opening and the ridge there was a narrow strip of ice to avoid the ridge mass spreading into the opening.

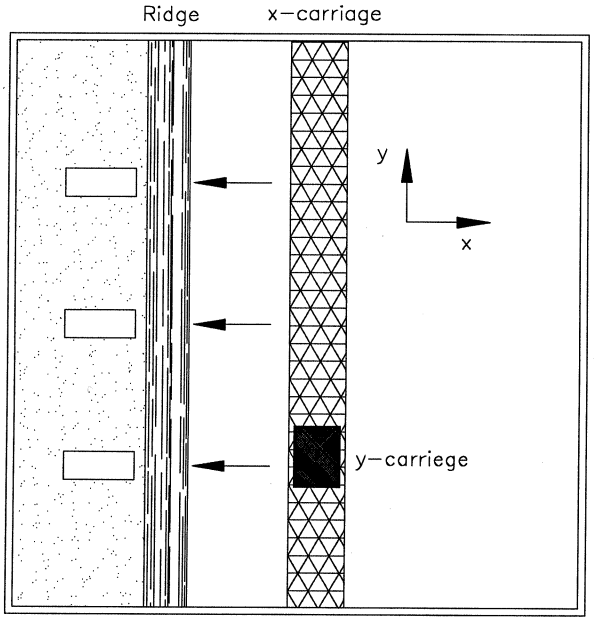

Figure 3: The test arrangements.

The geometry of the model ice ridges was defined by measuring the ridge thickness with an interval of 20 cm over the ridge from the side of each test location. In order to be able to compare the test results with an existing ridge resistance formula, some other ridge properties had to be defined.

The porosity of the ridge mass was determined from the ratio of the cross-sectional area of the ridge and the amount of ice used for the ridge. The coefficients of passive and lateral stress of the ridge mass were determined with a test where a vertical, rectangular indentor was pushed through the ridge with a constant speed and the indention force was measured. The passive stress was calculated with Equations 1 and 2 depending on the ridge thickness.

If $H_R \leq h_{IND}$,

$$P_p = \frac{F_{IND} H_R}{b_{IND}\ H_R} = \frac{\rho_\Delta \cdot (1-n) g H_R^2}{2} K_p, \tag{1}$$

and

if $H_R \geq h_{IND}$,

$$P_p = \frac{F_{IND} h_{IND}}{b_{IND} h_{IND}} = \frac{\rho_\Delta \cdot (1-n) g h_{IND} (2H_R - h_{IND})}{2} K_p \quad , \tag{2}$$

where H_R is ridge thickness, h_{IND} is the height of the indentor, F_{IND} is the indentation force, P_P is pressure, b_{IND} is the width of the indentor, ρ_Δ is the difference between the densities of water and ice, n is the porosity of ridge mass, g is the gravitational acceleration and K_P is the coefficient of passive stress.

The coefficient of lateral stress was calculated with Equation 3 (Helenelund 1981)

$$K_0 = 1 - \sin \phi_s, \tag{3}$$

where ϕ_s is the inner friction angle of the ridge mass from Equation 4

$$\begin{aligned} K_P &= \tan^2(45^\circ + \phi / 2) \\ \Rightarrow \phi &= 2(\arctan \sqrt{K_P} - 45^\circ). \end{aligned} \tag{4}$$

3 TEST RESULTS

The model tests were performed in six different ridges. If we assume that the resistance changes linearly in all phases in a five phased idealised resistance graph introduced in chapter 1, we can determine values for the maximum resistance and for the resistance components for the bow and parallel mid-body. These five phases were quite observable in the results of these model tests (Figure 4).

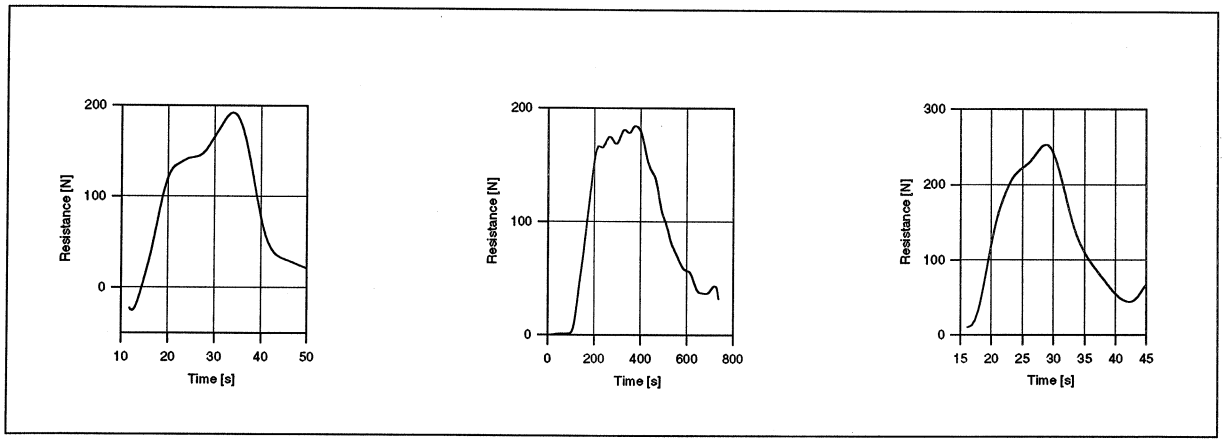

Figure 4: The filtered resistance graphs of three model tests.

The accuracy of the values for the different resistance components can be thought to be sufficient if we considered the inaccuracy of defining an ice ridge in nature. Figure 5 shows an idealised resistance graph together with a measured and filtered resistance graph.

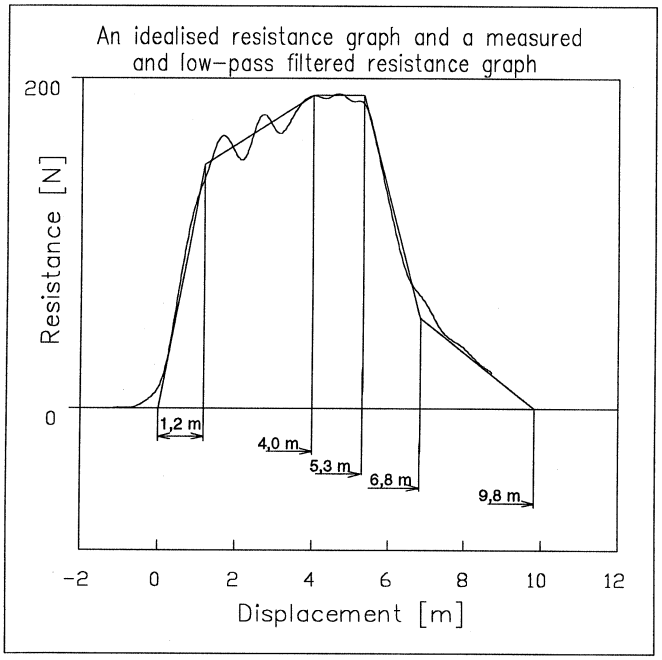

Figure 5: An idealised resistance graph and a measured and low-pass filtered (f=0.34 Hz) resistance graph.

In the idealised resistance graph the displacements corresponding to the phases come directly from the dimensions of the ship model and ridge length. Phase 1 corresponds to L_{bow}, phase 2 to L_{par}, phase 3 to L_R-L_{bow}-L_{par}, phase 4 to L_{bow} and phase 5 to L_{par}. The displacements in Figure 5, marked with arrows, correspond to the values 0.97 m, 4.10 m, 5.4 m, 6.37 m and 9.5 m, from the model and ridge parameters, respectively. Now the resistance for the bow of the ship R_{bow}, the resistance of the parallel mid-body R_{par} and the maximum resistance R_{max}

can be read as shown in Figure 1. The maximum total forces and their partitions between the resistance components for the bow and the parallel mid-body are presented in Table 1.

Table 1: Test results.

Test Number	Speed [m/s]	Cold sum [°Ch]	Average ridge thickness [m]	Measured Ridge Length [m]	Total Resistance [N]	Resistance components [N]	
						Parallel mid-body	Bow
1-1	0.01	0	0.34	3.2	184	37	147
1-2	0.46	0	0.30	3.4	263	80	182
2-1	0.23	0	0.35	3.4	233	66	167
2-2	0.23	18	0.33	3.2	250	45	205
2-3	0.23	35	0.32	3.2	289	50	239
3-1	0.23	0	0.33	4.0	260	68	192
3-2	0.23	19	0.32	4.4	260	60	200
3-3	0.23	39	0.35	3.6	288	56	232
4-1	0.23	0	0.32	3.4	253	45	208
4-2	0.23	18	0.32	4.0	275	45	230
4-3	0.23	70	0.33	3.6	310	73	237
5-1	0.23	0	0.21	5.2	192	45	147
5-2	0.23	22	0.23	5.4	192	38	154
5-3	0.23	39	0.21	5.4	175	41	134
6-1	0.23	0	0.22	5.4	178	43	135
6-2	0.23	28	0.24	5.4	174	41	133
6-3	0.23	48	0.23	5.4	237	75	162

3.1 The dependency of velocity

In the first ridge three different model velocities were used. The lowest velocity was 0.01 m/s which can be considered to be a zero speed, where there is no increase of the resistance caused by the velocity. Figure 6 shows the maximum resistance and the resistances for the bow and parallel mid-body as a function of speed.

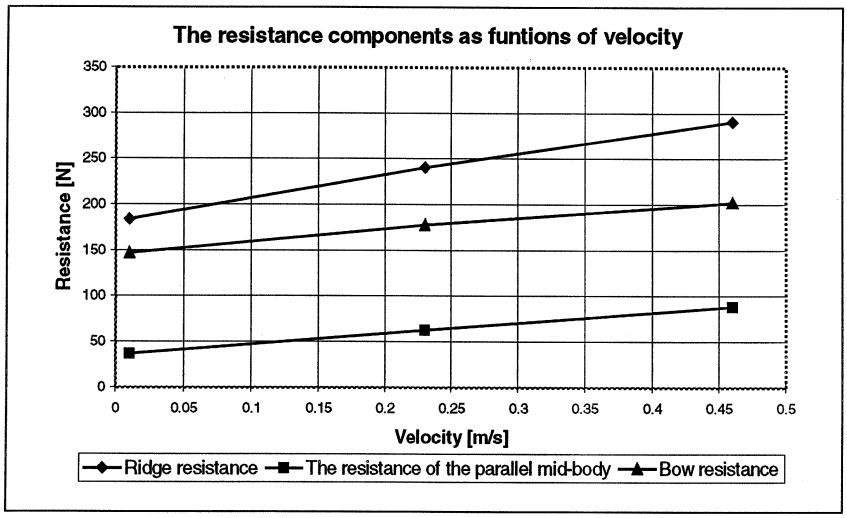

Figure 6: The values of the resistance component as functions of velocity.

Figure 6 shows that all three values increase as a function of ship's speed. If the resistance is thought to be a function of velocity of the form

$$R=C_1+C_2v^n, \qquad (5)$$

according to the test results, the exponent n seems to be very close to one and possibly less than one.

3.2 The consolidated layer

The influence of the consolidated layer on the resistance was studied in ridges 2...6. Only in ridge number 2 was the consolidated layer achieved by freezing the ridge without spraying. Ridges 2...4 were approximately of the same thickness and ridges five and six were thinner. The difference in the increase of the resistance between the sprayed and non-sprayed ridges when freezing was considerable. The resistance in the ridge that hadn't been sprayed was about 15 % lower when the ridges hadn't been frozen. When the ridges had been frozen about –40 °Ch the resistance in every ridge was very close to each other. All the tests were performed immediately after the freezing without tempering the layer. Figure 7 shows the resistance as a function of cold sum for one non-sprayed and two sprayed ridges. The effect of test methodology can also be seen.

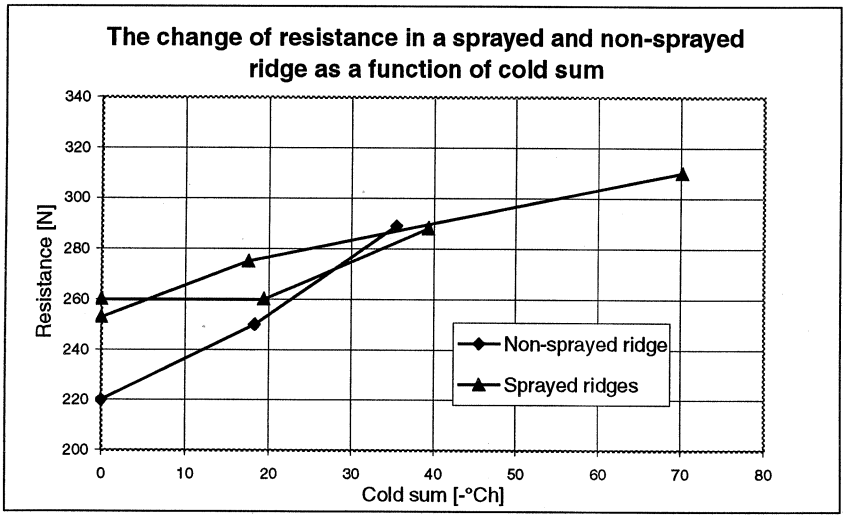

Figure 7: Resistance as a function of cold sum.

In the experiments the resistance of the parallel mid-body is 16 to 32 percent of the total resistance (Figure 8). The relatively large variation of the percentages depends slightly on the consolidated layer and other ridge characters, such as porosity. No significant difference between the thin and thick ridges can be seen. Usually, the thicker and harder the consolidated layer is, the lower is the part of the resistance for the parallel mid-body. Therefore the consolidated layer seems to have more influence on the resistance of the bow than the parallel mid-body. In these tests the effect of the consolidated layer was studied in general. The aim was to clear up the effect of the consolidated layer on the ratio of the components for the bow and parallel mid-body.

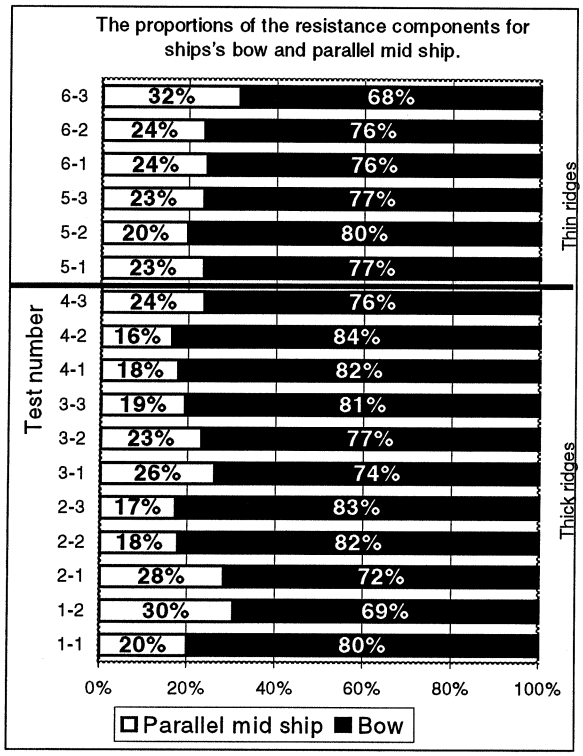

Figure 8: The division of ridge resistance.

4 DISCUSSION

If the model test results are compared with the results calculated with Equation 6 presented by Malmberg (1983), we can see that Malmberg's formula gives quite close resistance values for the bow but that the values for the parallel mid-body are far too small. In Malmberg's formula the first and second term present the resistance components at the bow and parallel mid-body respectively.

$$R_R = \rho_\Delta g T (1-n)\left\{ K_p H \left(\frac{1}{2} B + H \tan\psi \cos\alpha \right)(\mu_H \cos\phi + \sin\psi \sin\alpha) + \mu_H L_{par} \left(K_0 H + \left(\frac{H}{T} - \frac{1}{2} \right) B \right) \right\}, \quad (6)$$

where R_R is ridge resistance, n is the porosity of the ridge mass, ρ_Δ is the difference between the densities of water and ice, g is the gravitational acceleration, T is draught, K_p is the coefficient of passive stress, H is ridge thickness, B is beam, μ_H coefficient of friction between ice and the ship's hull, K_0 is the coefficient of lateral stress, L_{par} is the length of the parallel mid-body, α is the waterline entrance angle and ϕ is the stem angle. Angle ψ is determined in Equation 7.

$$\psi = \arctan\left(\frac{\tan\phi}{\sin\alpha} \right) \quad (7)$$

Table 2 gives the resistance values from the model tests and calculated with Malmberg's formula as well as the percentages of the resistance for the parallel mid-body.

Table 2: Comparison of the resistance values according to the model tests and Malmberg's formula.

	Model test results				Malmberg's formula			
Test	R_R [N]	R_{par} [N]	R_{bow} [N]	R_{par} [%]	R_R [N]	R_{par} [N]	R_{bow} [N]	R_{par} [%]
1-1	184	37	147	20%	148	14	134	9%
1-2	263	80	182	30%	175	10	166	6%
2-1	233	66	167	28%	161	13	149	8%
3-1	260	68	192	26%	140	9	130	7%
4-1	253	45	208	18%	183	10	174	5%
5-1	192	45	147	23%	149	3	146	2%
6-1	178	43	135	24%	133	4	129	3%

Malmberg's formula doesn't take the ship speed into account and so only the resistance values of test number 1-1 where the ship speed was only 0.01 m/s are relatively comparable.

4.1 Energy consumption

The energy consumption in the tests was calculated by integrating the resistance graphs as functions of the penetration distance (Izumiyama and Uto, 1995). When the model crosses the ridge from open water to open water, the energy consumed in the ridge is

$$E_R = \int_0^X R dx, \tag{8}$$

where R is resistance in ridge and X is the total displacement.

The connection of the energy consumption and the ridge parameters was studied by dividing the consumed energy by the maximum ridge resistance. The quotients were found out to be about the same magnitude as the ridge lengths. The product of the measured ridge resistance and the ridge length and the calculated energy consumption as well as their percentage difference are in Table 3.

Table 3: The comparison of the calculated energy consumption and product of the ridge length and maximim resisance.

Test Number	Calculated Energy Consumption [J]	Ridge Length x Max.Resistance	Difference [%]
1-1	685	589	-14%
1-2	954	893	-6%
2-1	765	792	4%
2-2	898	800	-11%
2-3	910	925	2%
3-1	991	1040	5%
3-2	1074	1144	7%
3-3	1080	1037	-4%
4-1	862	860	0%
4-2	1017	1100	8%
4-3	1192	1116	-6%
5-1	1129	998	-12%
5-2	885	1037	17%
5-3	985	945	-4%
6-1	1041	961	-8%
6-2	946	940	-1%
6-3	1550	1280	-17%

If we calculate the area of an idealised resistance graph we can see that the area is actually the maximum resistance multiplied by the length of the ridge (Figure 9).

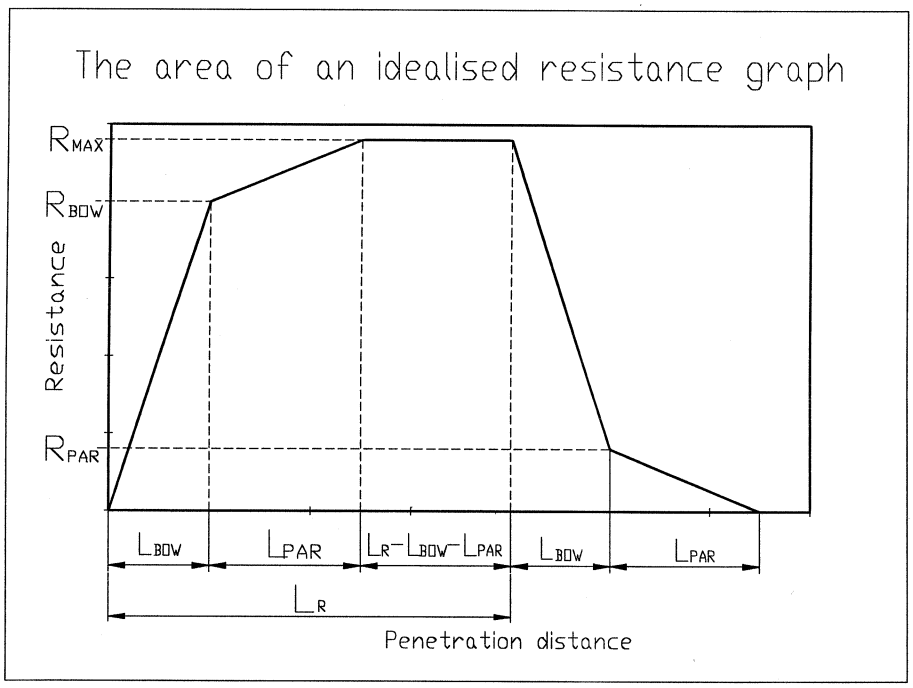

Figure 9: The area of an idealised resistance graph is the product of the maximum resistance R_{MAX} and the length of the ridge L_R.

5 SUMMARY AND CONCLUSIONS

The aim of this study was to study ship's ridge resistance and the ratio of the components for the bow and parallel mid-body in model scale. The ridge resistance and the resistances for the bow and parallel mid-body were defined through an idealised resistance graph that was constructed for each test. The proportion of the resistance component for the parallel mid-body was found out to be from 16 to 32 percent of the total resistance. The magnitude of the resistance values as well as the ratio of the component for the bow and parallel mid-body were compared with the corresponding values calculated with Malmberg's formula. For the resistance of the bow, Malmberg's formula gave results of the same magnitude as the model tests but for the parallel mid-body the values were too low.

The consumption of energy was also studied. For a simplified case where the ridge cross section is rectangular and the resistance graph is like the idealised resistance graph, the total energy consumption is the product of the ridge length and the maximum ridge resistance. According to the model tests where the cross section of the ridge was very close to rectangular the difference between the energy consumption calculated, as a product of the ridge length and maximum resistance, and that integrated from the resistance graph varied between –17 and +17 %.

6 ACKNOWLEGEMENTS

This work was done as a Master Thesis at the Helsinki University of Technology under the supervision of Professor Kaj Riska and under instruction of Dr. Jukka Tuhkuri.

7 REFERENCES

Helenelund, K.V. 1981. Soil Mechanics. Espoo. Otakustantamo. 278 p. (In Finnish).

Izumiyama, K.; Shotaro, U. 1995. Ice Resistance of Three Bow Forms for the NSR Cargo Ship. IST'95, INSROP Symposium. Tokyo, pp 459-467.

Leppäranta, M.; Hakala, R. 1992. The Structure and Strength of First-year Ice Ridges in the Baltic Sea. Cold Regions Science and Technology. 20, pp. 279-290.

Li, Z.; Riska, K. 1996. Preliminary Study of Physical and Mechanical Properties of Model Ice. Espoo, Helsinki University of Technology, Ship Laboratory, report M-212. 100 p + App.

Malmberg, S. On the Mechanism of Getting Stuck in Ice. 1983. M. Sc. Thesis. The Department of Mechanical Engineering. Helsinki University of Technology. Espoo. 69 p. (In Swedish).